Journal of Fluid Science and Technology

Vol. 3, No. 5, 2008

A Method for Visualization of Brain Neural Pathway Using Critical Points and Target Regions*

Akio DOI**, Hironori FUJIMURA***, Masaki NAGANO**, Takashi INOUE**** and Akira OGAWA****

* *Iwate Prefectural University, 151-52 Sugo, Takizawa-mura, Iwate, Japan
E-mail: doia@soft.iwate-pu.ac.jp

*** Alps Corporation, 5-4-12 Nishi-hashimoto, Sagamihara-shi, Kanagawa, Japan

****Iwate Medical University, 19-1 Uchimaru, Morioka-shi, Iwate, Japan

Abstract

Visualization of a brain neural pathway is a useful tool for supporting surgical planning. In this paper, we propose a method for visualizing a brain neural pathway by using both critical points and target regions in order to extract necessary pathways. Here, critical points are those points at which the magnitude of the vector vanishes, and we assume that a neural pathway consists of a set of streamlines in a vortical flow field and we find the start points of streamlines by classifying critical points. The user also specifies target regions, such as regions of interest, and visualizes the important streamlines that pass through the target regions.

Key words: Visualization, Brain Neural Pathway, Critical Points, Region of Interest (ROI), Streamlines, Target Regions, Tractography

1. Introduction

Brain neural pathway visualization using diffusion tensor-magnetic resonance imaging (DT-MRI) is used in the early detection of illnesses, as well as in the support of both surgical and post-surgical planning. Fig. 1 shows a visual representation of neural pathways in the brain, treated with special chemicals to make pathways visible to the naked eye [(1)]. DT-MRI produces multiple 3-dimensional images by applying magnetic fields from multiple directions (6 directions in this research). Directions of fiber in brain white matter influence the movement of water molecules, and signal strength changes according to the relationships between the magnetic field gradient in the diffusion direction and the direction of the pathway. Water molecule diffusion perpendicular to the direction of the white matter pathway is low in comparison to diffusion in a parallel direction [(2)].

Several major differences between the directions of fiber in brain white matter and flow fields in computational fluid dynamics have been identified:

1) Discontinuities exist in flow fields when neural pathways intersect (Partial Volume Effect).
2) The important neural pathways within the brain must be shown anatomically.
3) Greater distortions and errors exist near bones, which are less affected by magnetic fields.
4) Image noise influences the direction of brain pathways.

*Received 15 Jan., 2008 (No. 08-0024)
[DOI: 10.1299/jfst.3.678]

Therefore, many tractography methods for DT-MRI have been proposed in relation to tracking from seed points, seed specifications, terminating conditions, and so on. Most tractography methods use the major diffusion tensor eigenvector to define local fiber direction; the first tract points are specified in brain regions and then geometry primitives, such as streamlines, stream tubes, and arrow plots, are displayed [3]-[7]. The start points of tractography are generated by seeding specified brain regions [3], [4], or seeding large regions of the brain [7].

Critical points are those points at which the magnitude of the vector vanishes, and we use information of critical points as the start points of streamlines [8]. We classify each critical point as a saddle point, attracting node/focus, repelling node/focus, or center. We use the position of these critical points except the saddle points in our method. The classification can be done by using real and imaginary parts of eigenvalues of the Jacobian matrix at the critical point [10], [11].

More concretely:

- Appropriate start points of streamlines are located by considering the fractional anisotropy (FA) values of point groups near critical points.
- From streamlines that pass near critical points, those passing through important regions are extracted and colored appropriately to clearly display the directions of neural pathways.
- In addition to plane regions and rectangular regions, volume regions which are important in anatomy, such as the cerebral peduncle, can be specified.

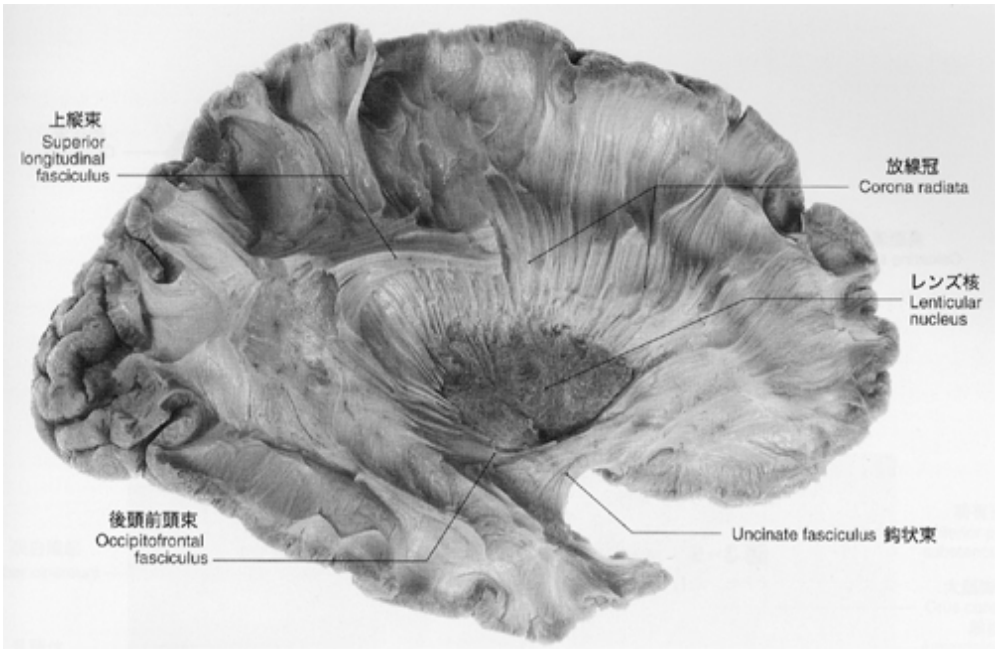

Fig. 1 Naked eye view of neural pathways

Specialized knowledge is normally required to select the start points of streamlines interactively in order to display important neural pathways of grey and white matter. This interactive operation is also extremely time consuming [9]. In addition, when extracting streamlines from the specified start point region, a number of similar pathways will be visualized, and it is difficult to distinguish important pathways. Furthermore, when neural pathways separate in multiple directions from a start point, pathways can generally only be followed in a single direction. To resolve these issues, the start points (critical points) of the

neural pathway are automatically calculated first. Then the streamlines passing near those start points are calculated, and only those streamlines passing through the target region are displayed (extracted).

In order to specify target regions that pass through important neural pathways, we prepare two approaches for users. The first approach is to use interactive methods. The user paints them slice-by-slice or on a per- voxel basis. The second approach is to use segmentation methods. The user can use a region growing method, a watershed method, image filtering, or histogram-based selection. The information for the target regions is stored as a mask image. Next, each neural pathway that passes through each target region is colored. In this paper, Section 2 discusses the extraction of neural pathways and critical points, Section 3 deals with algorithms to follow neural pathways, Section 4 presents applications and an evaluation of our algorithm, and Section 5 covers the conclusions and future issues.

2. Critical Points and Neural Pathways

Generally, the direction of neural pathways is stored as tensor data after being deduced by diffusion strength for each direction from MRI and DT-MRI signals. This data is diagonalized, and from the 3 eigenvalues obtained, we presume that the eigenvector with the largest eigenvalue represents the main direction of the neural pathway. At this point, there is no indication of whether the direction of the eigenvector is positive or negative, so both possibilities must be considered.

To display the streamlines, the user first selects a start point, and the tangent curves at the position are approximated as straight lines. Tri-linear interpolation of the 8 vertices of the voxel [9] is used for the integration. The termination condition is determined when a predetermined number of steps is reached, or when the direction value becomes a threshold value (such as 10^{-7}), or when error processing is continued for a pre-determined number of iterations [11), (17)].

Start points are selected interactively, and the necessary pathways are extracted. To display the pursuit results, FA values (a measure of the degree of diffusion) are used to color code pathways. FA values range between 0.0 and 1.0, representing a degree of anisotropy, with higher values representing higher diffusion differences in each direction. FA is defined in the following formulae:

$$\mathrm{FA} = \sqrt{\frac{3}{2}\,\frac{(\lambda_1-\mathrm{D})^2+(\lambda_2-\mathrm{D})^2+(\lambda_3-\mathrm{D})^2}{\lambda_1^2+\lambda_2^2+\lambda_3^2}} \qquad (1)$$

$$\mathrm{D} = \frac{\lambda_1+\lambda_2+\lambda_3}{3} \qquad (2)$$

where, λ_1, λ_2, and λ_3 are eigenvalues of the diffusion tensor, and D is averaged diffusion

In the visualization of flow fields, the locations of vortex centers (where speed = 0) offer important guides. The eigenvalue of the diffusion tensor in each voxel is obtained from DT-MRI, and the eigenvector for the highest eigenvalue of this group is calculated. This eigenvector can be assumed to be the direction of flow, allowing critical points to be identified. In the critical points calculation used in this paper, the voxel with 8 vertices is divided into 5 tetrahedra, and location of critical points for each tetrahedron is calculated. This calculation does not require numerical methods, such as the Newton-Raphson method. We can calculate critical points for each tetrahedron by using a cubic linear equation [12].

Generally, if we simply use critical points as the start points for neural pathway directions, due to the nature of DT-MRI, a large number of critical points will be identified, and an extremely confusing image would be produced. Fig. 2 shows 256 x 256 x 60 data from a healthy patient, with the critical points highlighted in red. Fig. 3 shows an image of the results of calculating all the streamlines neighboring the critical points found in Fig. 2. We use position of the attracting node, attracting focus, repelling node, repelling focus, and center for critical points; we do not use saddle points.

3. Proposed Method

3.1 Overview

Our algorithm to follow neural pathways is shown in Fig. 4. We assume that brain neural pathways consist of streamlines in flow fields. We calculate the critical points and specify the locations with high FA values in that area as the start points of the streamlines. By displaying those streamlines that pass through the target region as selected by the user, important neural pathways can be displayed in an easily understandable manner. Critical points are important guides in understanding the characteristics of flow fields [8], [10]. We take the centers of the 26 proximity voxels neighboring a voxel containing a critical point as candidates for the start points of the streamlines.

From among these candidates, locations with high FA values (where there is a high possibility of a pathway being present) are set as the start points of the streamlines. Here, the FA value should be 0.5 or higher.

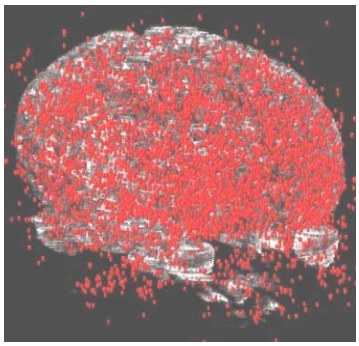

Fig. 2 Searched critical points

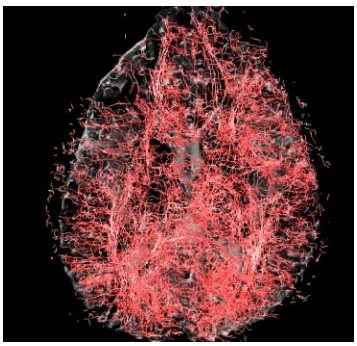

Fig. 3 Streamlines from critical points

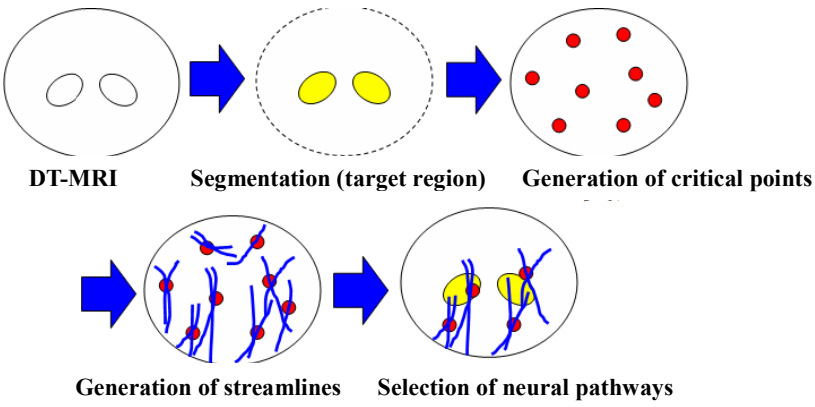

Fig. 4 Overview of our algorithm

3.2 Setting Target Regions

Following all of the critical points acquired as described in Section 3.1 results in an extremely high number of overlay pathways being extracted. The next step is thus to extract those pathways that pass through a specified region. To extract the necessary pathways, Sherbondy et al. set region of interests (ROIs), such as rectangular target regions, and only displayed those pathways that pass through these regions [13].

In addition to specifying rectangular target regions, we propose a flexible method of specifying ROIs. We extract specified areas in the form of arbitrary multiple volume regions and designate them as target regions. These regions are extracted through a combination of a segmentation technique, such as a region growing method, a histogram based segmentation method, or an interactive segmentation method. This information is stored in binary mask images [11], [17].

Fig. 5 shows a neural pathway that is selected by using a target region from the neural pathways shown in Fig. 3. Outlines of the crus posterius capsulae internae, cerebral peduncle, and meningioma were extracted interactively by selecting a 2-dimensional X-Y slice. The tool used was Volume Extractor Ver. 3.0 software that we have developed at our university [14].

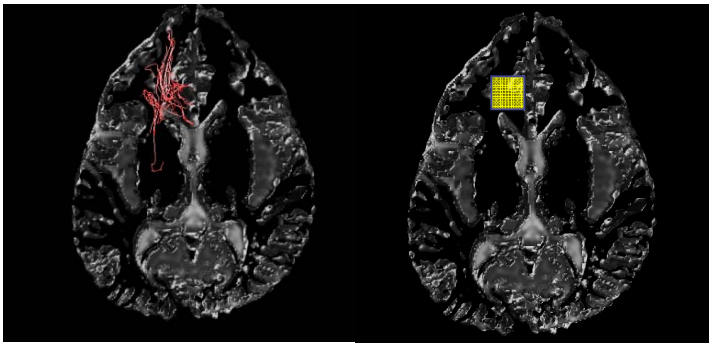

Fig. 5 Selection of neural pathways using a target region (yellow box)

3.3 Dealing with Intersections

Out of the 3 eigenvectors obtained, the vector that represents the primary direction alone is used for following the pathways. For this reason, when pathways intersect, only the pathway in the primary direction is followed. In the method presented here, when an intersecting pathway is encountered, the direction just prior to the intersection is used, thus resolving this issue. In this manner, the angle of approach is undamaged and the intersecting pathway can be followed.

Note that intersecting points are determined by their low FA values (0.2 or less). Intersecting points feature multiple pathways in various directions, so the difference of the eigenvalues decreases and the FA value becomes smaller. In addition, neural pathways are assumed not to suddenly turn at sharp angles, and if the difference in angle between direction A obtained before the intersection and direction B obtained at the intersection is over a certain range (60°), direction A is used.

3.4 Coloration

An educational model of brain neural pathways that is used in hospitals to explain surgery to patients has each region of the neural pathways colored, making pathways easy to distinguish (Fig. 6). As shown in Fig. 6, neural pathways at each region should be colored, making important pathways easy to distinguish. Generally, pathways are color coded according to direction or FA values. In such cases, it is difficult to represent different important pathways.

The left and right images of Fig. 7 show an example of an ordinary coloration using FA values and our coloration using target regions, respectively. Fig. 8 shows another example of our coloration method. To create this kind of brain neural pathway model, each target region is assigned a separate, distinguishable ID. Next, assuming that the pathways pass through multiple target regions, 2^x-1 tables are created containing the color or other identifying information (where x represents the number of selected target regions).

For example, if 2 target regions (o_1, o_2) are used, the pathways can be separated into 3 groups based on which target region they pass through, (o_1), (o_2) and (o_1, o_2), and are assigned a number accordingly and colored. If 3 target regions (o_1, o_2, o_3) are used, then the combinations are (o_1), (o_2), (o_3), (o_1, o_2), (o_1, o_3), (o_2, o_3) and (o_1, o_2, o_3). A color is determined by referring to the table while assigning color information to each pathway number.

Fig. 6 An educational model of brain neural pathways

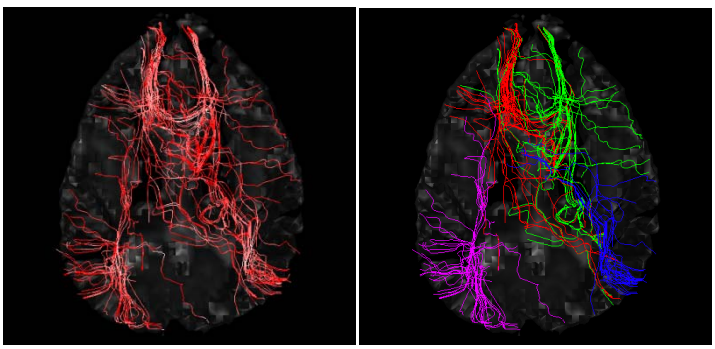

Fig. 7 Coloration of the brain pathway using FA values (left) and target regions (right) (xy plane)

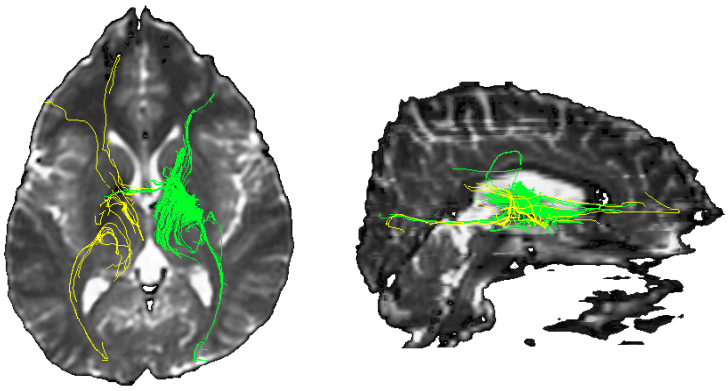

Fig. 8 Coloration of the brain pathway using target regions (xy and yz plane)

4. Application and Evaluation

4.1 DT-MRI and Experiments

Two DT-MR images, created by applying a magnetic field from 7 directions were used in this experiment. The resolution is 256 x 256 x 60. One DT-MR image is of a healthy 19-year-old woman, and the other is of a 53-year-old female patient with meningioma. The equipment used is an MR Scanner (GE-Medical) with 3-T magnetic fields, and a gradient magnetic field factor b of 800 s/mm^2. Tri-linear interpolation was used to transform this data into 60 x 60 x 60 isotropic voxels.

It is not effective to calculate all streamlines from all critical points, as shown in Fig. 2, because it is difficult to distinguish the important neural pathways. To resolve this issue, target regions through which important brain neural pathways pass are set. In this research, the crus posterius capsulae internae and meningioma areas were selected as the target regions. Of the pathway groups pursued from near critical points, only those passing through this target region were displayed (Fig. 5). The pathways in Fig. 8 are not color coded by FA value but by whether they pass through the left or right crus posterius capsulae internae.

Fig. 9 shows an MRI slice image from the meningioma patient, with the white area on the left identified as an abnormality. In Fig. 10, the region around the meningioma was selected as the target region, and only those pathways passing through this region were displayed. These are superimposed on MRI, and the area around the tumor is color coded yellow, making it easier to grasp the relative locations of the brain and the tumor. A layered display of the cerebral nerve was created using AVS/Express version 7.0 visualization software.

4.2 Computational Processing Time

This section describes the processing time taken by this method. The operating system used in this research is Windows XP, running Visual C++ version 6.0. The hardware used consists of a 1.50 GHz Pentium M CPU with 1.25 GB of RAM. Eigenvalues and eigenvectors were calculated using the Jacobi method [15]. Three types of processing time comparison were performed: processing time by specified regions with neural pathways passing through; processing time by data size; and processing time when critical points are used as start points and when they are not. The left and right of the crus posterius capsulae internae and cerebral peduncle of the healthy patient were selected as target regions by

using a medical book of anatomy and physiology [16]. With data obtained from the meningioma patient, the area around the tumor was selected.

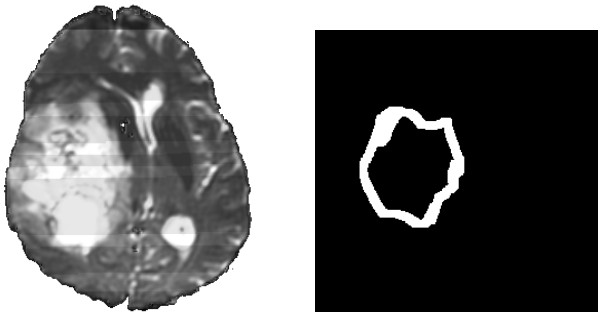

Fig. 9 MRI of meningioma patient and target region

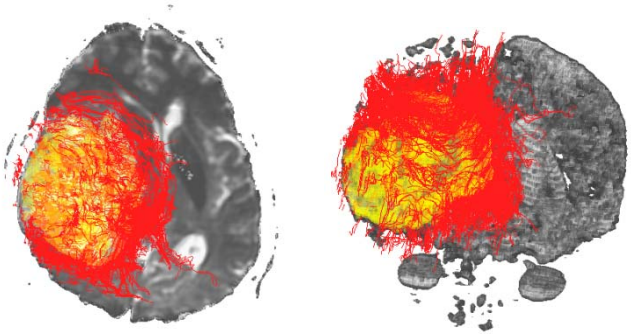

Fig. 10 Results of brain pathway pursuit (xy plane and 3D display)

Table 1 shows the computational time for each data set in which the target region is set. The "Crus posterius", "Cere. peduncle", and "Tumor area" represent the crus posterius capsulae internae, cerebral peduncle, and area around tumor (meningioma), respectively. As a pre-process, the diffusion direction of each pixel is deduced from the acquired DT-MRI and written to a file. After reading the file, all critical points are calculated. The extracted neural pathways are written to an external file. The time taken to pursue neural pathways and all other times (reading and writing files, extracting critical points) were totaled separately. All times are measured in seconds. The alphabetic code assigned in Table 1 corresponds to the following resolutions and patient data. The third number shows CPU search time for critical points (seconds) and the fourth number shows the number of critical points.

- A: 256x256x60 data from healthy patient: 32.1 sec. (CPU search), 6448 (critical points)
- B: 60x60x60 data from healthy patient: 3.8 sec., 405
- C: 256 × 256 × 240 data of healthy patient: 101.0 sec., 20037
- D: 256 × 256 × 60 data of meningioma patient: 27.2 sec., 5148
- E: 60 × 60 × 60 data of meningioma patient: 3.5 sec., 401
- F: 256 × 256 × 240 data of meningioma patient: 92.8 sec., 17757

Table 2 shows the number of critical points by data size. The number of critical points is increased in proportion to data size, and the points are searched with similar precision. Table 3 compares pathway data extracted under this method.

In the "No. of Pathways" column in the table, for a given start point, pathways followed in a

positive and negative direction are counted once. The "No. of Steps" column shows the number of iteration steps used to extract the pathways. The value shows the total number of steps for neural pathways passing through the target regions. Finally, the "File Size" column represents the size of the AVS/Express output file (file format: inp) produced by saving pursuit results, measured in megabytes.

As shown in Table 1, if the selected target region is small, pursuing neural pathways directly from the target regions is more effective than pursuing them from the critical points. However, when the target region is large, as with the area around the meningioma, pursuing the neural pathways becomes increasingly time consuming, and in such a case, extracting those neural pathways from around the critical points is faster.

As shown in Table 2, when dealing with DT-MRI, we can see that a large number of critical points are created when image data includes noise. By selecting only the important critical points ahead of time, calculation time can be reduced. The target regions were interactively specified as 3-dimensional target areas (volume region). Segmentation of the crus posterius capsulae internae and cerebal peduncle, as in this example, can be relatively clearly imaged using MRI, and since the number of slices is low, its extraction is relatively easy.

Table 1 Comparison of computational time (seconds)

Data	Start Point	Target Region	Pursuit Time	Other	Total
A	Crus posterius	None	4.797	13.457	18.254
A	Critical point	Crus posterius	60.984	49.631	110.615
A	Cere. peduncle	None	4.133	13.301	17.434
A	Critical point	Cere. peduncle	44.754	49.875	94.629
B	Crus posterius	None	0.150	1,034	1.184
B	Critical point	Crus posterius	1.579	5.832	7.410
B	Cere. peduncle	None	0.170	0.874	1.044
B	Critical point	Cere. peduncle	0.921	4.830	5.751
C	Crus posterrius	None	102.381	56.019	158.400
C	Critical point	Crus posterius	505.053	164.895	669.948
C	Cere. peduncle	None	97.467	56.384	153.851
C	Critical point	Cere. peduncle	410.393	165.759	576.152
D	Tumor area	None	2301.456	68.585	2370.041
D	Critical point	Tumor area	1136.915	55.432	1192.347
E	Tumor area	None	3.945	2.948	6.893
E	Critical point	Tumor area	7.147	5.538	12.685
F	Tumor area	None	22322.270	238.684	22560.957
F	Critical point	Tumor area	14285.287	170.990	14456.277

Table 2 Comparison of streamlines

Data	Start Point	Target Region	No. of Pathways	No. of Steps	File Size (M bytes)
A	Crus posterius	None	2031	95533	7.5
A	Critical point	Crus posterius	697	75063	5.8
A	Cere. peduncle	None	1324	89140	7.0
A	Critical point	Cere. peduncle	1030	83653	6.5
B	Crus posterius	None	242	11357	0.9
B	Critical point	Crus posterius	146	15725	1.1
B	Cere. peduncle	None	76	4938	0.4
B	Critical point	Cere. peduncle	96	8116	0.6
C	Crus posterius	None	8658	462835	38.7
C	Critical point	Crus posterius	820	93576	22.2
C	Cere. peduncle	None	6868	454246	37.5
C	Critical point	Cere. peduncle	1948	183191	14.6
D	Tumor area	None	70255	2174398	190.0
D	Critical point	Tumor area	13165	539331	43.8
E	Tumor area	None	5284	85586	6.93
E	Critical point	Tumor area	1808	41122	3.08
F	Tumor area	None	271446	6701121	610.0
F	Critical point	Tumor area	36952	643714	52.8

5. Conclusion

In this research, brain neural pathways were pursued using critical points as start points, and pathways passing through target regions were extracted. Using the proposed coloration method, neural pathways are easily distinguished, such as by color coding the left and right crus posterius capsulae internae separately (Fig. 8). In addition, data from a patient with a meningioma were used in this study to show the potential usefulness of this method in surgical planning. By setting an area around the tumor as a target region, the distribution of neural pathways around tumor provides effective and helpful information to doctors and patients.

In Fig. 10, pathways avoiding the meningioma were extracted, and accurate pursuit results were obtained. If the area of the target region is large, then processing capacity is improved using this method compared to pursuing neural pathways from the target region. However, if the target region is small, such as the crus posterius capsulae internae, then extracting pathways directly from the target region may be faster. In such cases, pathway pursuit results do not differ greatly from the method using critical points.

The recent progress of MRI hardware makes it possible to increase both the resolution of DT-MRI and the image capture speed. In addition, several new approaches for image capture [18], [19] and for fiber tracking [20], [21] have been proposed. These research results and the latest advances in MRI hardware will also improve our fiber tracking results.

Considering the future prospects of the proposed method, the pathway pursuit results do not seem to be sufficiently accurate at present. More accurate extraction of neural pathways from points where pathways intersect is needed. In addition, to reduce the burden placed on the user, the current methods of manual segmentation must be automated. In the present research, this method was applied to the area around the meningioma, allowing the region around the borderline to be clarified. In future, this method based on the direction of neural pathways must be applied to predicting the border areas of gliomas where such detection is difficult. In addition, interrelationships between neural pathways and blood vessels and the visualization of this relationship remains a very interesting issue to pursue.

Acknowledgements

We would like to extend our deep thanks to Mr. Yoshiyuki Kanbara of Iwate Medical University Isotope Center for the many words of advice and for cooperation in gathering data. We would also like to sincerely thank Prof. Koji Koyamada and Prof. Koji Sakai of Kyoto University for their valuable opinions and advice.

References

(1) Haines, D. E. (Yamauchi, A.: Translation), Haines Neural Pathway Anatomy Atlas Second-edition, Medical Science International, 2003.
(2) Aoki, S., Abe, O., & Masutani, Y., Easy Understanding of Diffusion MRI (Korede Wakaru Diffusion MRI), Shuei-sha, 2002.
(3) Mori, S., Crain, B., Chacko, V. P., & van Zijl, PCM, Three Dimensional Tracking of Axonal Projections in the Brain by Magnetic Resonance Imaging, Annals of Neurology, Vol. 45, No. 2, pp. 265-269, 1999.
(4) Basser P. J., Pajevic S., Pierpaoli C., Duda J., & Aldroubi A., In Vivo Fiber Tractography Using DT-MRI Data, Magnetic Resonance in Medicine, Vol. 44, pp. 625-632, 2000.
(5) Basser, P. J., Pajevic, S., Pierpaoli, C., & Aldroubi, A., Fiber Tract Following in the Human Brain Using DT-MRI Data, IEICE Trans Information Sys, E85D, pp. 15-21, 2002.
(6) Barr, H. A., Oriented Tensor Reconstruction: Tracing Neural Pathways from Diffusion Tensor MRI, IEEE Visualization 2002, pp.387-394, 2002.
(7) Conturo, T. E., Lori, N. F., Cull, T. S., Akbudak, E., Snyder, A. Z., Shimony, J. S., McKinstry, R. C., Burton, H., & Raichele, M. E., Tracking Neuronal Fiber Pathways in the Living Human Brain, Proc. of National Academy of Sciences, Vol. 96, No.18, pp. 10422-10427, 1999.
(8) Helman J. L. & Hesselink, L., "Representation and Display of Vector Field Topology in Fluid Flow Data Sets ", Vol. 22, Issue 8, pp. 27-36, IEEE Computer, 1989.
(9) Volume-One, http://www.volume-one.org/dTV
(10) Sakai, K., A Study of Visualization Techniques based on Critical Points, Iwate Prefectural University, Faculty of Information and Computational Science, doctorial paper, 2004.
(11) Fujimura, H., Sai Y., Mochizuki T., Doi, A., Inoue, T., Sasaki, M. & Ogawa, A., Visualization of Brain Neural Pathway by Using Streamlines, Japan Visualization Symposium, Vol. 25, No. 1, pp.1-8, 2005.
(12) Doi, A., Suzuki, S., Koyamada K. & Sannakanishi, S., Vortex Flow Visualization using

Tetrahedral Subdivision – Improved Method and Its Applications, Journal of the Institute of Image Electronics Engineers of Japan, Vol. 26, No. 4, pp. 333-340, 1997.
(13) Sherbondy, A., Akers, D., Macenzie, R., Doughety, R., & Wandell, B., Exploring Connectivity of the Brain's White Matter with Dynamic Queries, IEEE Trans. on Vis. and Computer Graphics, Vol. 11, No. 4, pp. 419-430, 2005.
(14)Volume Extractor Ver.3.0, 3D Volume Visualization System, http://www.i-plants.jp/hp/products/ve3/
(15) Press, W. H., Flannency, B. P., Teukolsky, S. A. & Vetterling, W. T., Numerical Recipes in C: The Art of Scientific Computing, Cambridge University Press, 2004.
(16) Hinohara, S., Abe, M., Asami, K. & Seki, Y., Systematic nursing art and science lecture special basic 1, Human structure and its functions, anatomy and physiology, Igaku-shoin Ltd, 1999.
(17) Doi A., Fujimura H., Nagano M., Inoue T., & Ogawa A., A Method of Visualization of a Brain Neural Pathway by Using Critical Points and Target Regions, Modeling in Medicine and Biology 7, pp. 309-318, WIT Press, 2007.
(18) Frank, L. R., Anisotropy in High Angular Resolution Diffusion-Weighted MRI, Magnetic Resonance in Medicine, Vol. 45, No. 6, pp. 935-939, 2001.
(19) Tuch, D. S., Q-ball Imaging, Magnetic Resonance in Medicine, Vol. 52, No. 6, pp. 1358-1372, 2004.
(20) Masutani, Y., Aoki, S., Abe, O., & Ohtomo, K., A New Fiber Tracking Method based on Vector Field Reconstruction Excepting Fiber Crossing Area in MR Diffusion Tensor Images, Medical Imaging Technology, Vol. 22, No. 5, pp. 243-249, 2004.
(21) Cheng, P., Magnotta, V. A., Wu, D., Nopoulos, P., Moser, D. J., Paulsen, J., Jorge, R., & Andreasen, N. C., Evaluation of the GTRACT Diffusion Tensor Tractography Algorithm: A Validation and Reliability Study, Neuroimage, Vol. 31, No. 3, pp. 1075-1085, 2006.